CrossMark

TECHNICAL PAPER

Simplified precise model of Reynolds equation for simulating ultra-thin gas film lubrication in hard disk drives

Bao-Jun Shi[1,2] · **Yu-Jie Feng**[1] · **Jia-Dong Ji**[1,3] ·
Longqiu Li[2] · **Chuanwei Zhang**[2]

Abstract In order to increase the recording density of magnetic disk drives, the spacing between the flying head and the rotating disk must be as small as possible. When the spacing between the flying head and the rotating disk approaches the mean-free path of the gas, rarefaction effects must be taken into account. The authors propose a simplified precise second order (PSO) model that implements a Poiseuille flow rate database to simulate ultra-thin gas film lubrication. The PSO model is evaluated using the finite volume method. Numerical results obtained using the PSO model are presented and compared with the results from simulations that implement four formerly and currently employed lubrication models including the first-order, the second-order, the 1.5-order, and the widely used FK (Fukui and Kaneko) models. The PSO model's key advantages are validated in three aspects: mathematical formulation, simulation accuracy, and computational efficiency.

1 Introduction

In order to increase the storage density of magnetic disk drives, the reduction of the spacing between the slider and the rotating disk is of great importance. If the spacing

✉ Bao-Jun Shi
  shibj2003@126.com

1 School of Mechanical and Electronic Engineering,
   Shandong Jianzhu University, Jinan 250101, China

2 Center for Magnetic Recording Research,
   University of California, San Diego, CA 92093, USA

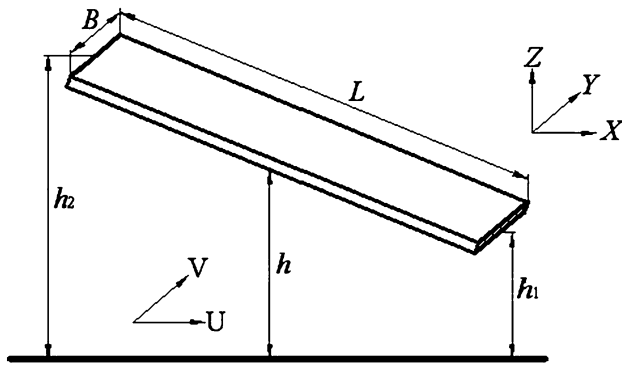3 School of Mechanical Engineering, Shandong University,
   Jinan 250061, China

between the slider and the disk approaches the molecular mean-free path of the gas medium, continuum theory cannot be used anymore (Burgdorfer 1959; Hsia and Domoto 1983; Juang et al. 2007; Liu et al. 2007). In present hard disk drives (HDDs), the minimum spacing under the slider has decreased to the order of several nanometers (<5 nm) (Liu and Zheng 2011; Zheng et al. 2012; Salas and Talke 2013). Under such conditions, gaseous rarefaction effects cannot be neglected and must be taken into account.

In order to account for rarefaction effects, several researchers introduced slip correction models for use in conjunction with the generalized Reynolds equation. Burgdorfer (1959) applied a first-order slip-flow correction to the non-slip continuum boundary condition. Hsia and Domoto (1983) derived a modified Reynolds equation that considers both first and second order slip flow for the velocity boundary conditions. Mitsuya (1993) introduced a 1.5-order slip flow model that uses different order slip boundary conditions for the integration of the isothermal compressible Navier–Stokes equations. The three slip-flow models proposed by Burgdorfer, Hsia and Domoto, and Mitsuya are only valid for large inverse Knudsen numbers, where the Knudsen number is defined as λ/h (λ is the molecular mean-free path of the gas medium and h is the head/disk interface spacing). Gans (1985) derived a lubrication equation using a linearized Boltzmann equation similar to Burgdorfer's modified first-order Reynolds equation and claimed that the linearized equation is valid for all inverse Knudsen numbers. Fukui and Kaneko (1988) derived a generalized Reynolds equation that includes thermal creep flow. This equation is based on a linearized Boltzmann equation similar to Gans' equation but implements a different solution method. Fukui and Kaneko (1990) proposed a cubic polynomial curve fitting procedure which creates a

Fig. 1 Geometry of two dimensional inclined plane slider bearing and coordinate system employed

2 Reynolds equation and simplified model

For a two dimension (2D) plane air bearing slider as shown in Fig. 1, the generalized non-dimensional 2D-Reynolds equation based on the FK model (Fukui and Kaneko 1990) is as follows:

$$
\begin{cases}
\dfrac{d}{dX}\left(QPH^3\dfrac{dP}{dX} - \Lambda_x PH\right) + \dfrac{d}{dY}\left(QPH^3\dfrac{dP}{dY} - \Lambda_y PH\right) = 0 \\
Q = \dfrac{Q_p(D,\alpha)}{Q_{con}(D)} \\
\Lambda_x = 6\mu UL/(p_a h_1^2), \ \ \Lambda_y = 6\mu VB/(p_a h_1^2) \\
H(X) = 1 + \dfrac{L}{h_1}(1-X)\tan(\theta)
\end{cases}
\tag{1}
$$

where P and H are the non-dimensional pressure and spacing, respectively. P is normalized by the ambient pressure (p_a) and H is normalized by the minimum spacing at the trailing edge of the slider (h_1). X is the coordinate along the length of the slider and Y is the coordinate along the width of the slider. L and B are the length and width of the slider, respectively. Λ_x and Λ_y are the bearing numbers in the X and Y directions, respectively. The dynamic viscosity of the gas is given by μ. θ is the pitch angle of the slider, and U and V are the disk velocity in the X and Y direction, respectively. Q is the flow factor accounting for difference between different rarefaction and slip models. $Q_p(D, \alpha)$ is the Poiseuille flow rate coefficient, and $Q_{con}(D)$ is the coefficient of continuum flow. Quantities D and α are the inverse Knudsen number and the surface accommodation coefficient, respectively. The definition of D and Q_{con} is as follows:

$$
D = D_0 PH = ph/(\mu/\sqrt{2RT})
\tag{2}
$$

$$
Q_{con} = D/6
\tag{3}
$$

where, D_0 denotes the inverse Knudsen number of the gas film at the minimum spacing, T is the characteristic temperature, and R is the gas constant.

The flow factor can be calculated from flow rate coefficients that are expressed in the form of a power series. For small inverse Knudsen numbers (D), where the slip flow assumption is reasonably valid, an asymptotic expression for $K_n \gg 1$ can be employed. Power series representations for $0.15 \le D \le 5$ and $0.01 \le D < 0.15$ can be calculated using the least squares method. The Poiseuille flow rate coefficient (Q_p) of the FK model are as follows (Fukui and Kaneko 1990):

function that explicitly expresses the Poseuille flow rate as a function of the inverse Knudsen number. From this expression they developed a Poiseuille flow rate database. Fukui and Kaneko' model will be referred to as the FK model in this paper. In order to overcome complicated and time-consuming difficulties found in solving the linearized Boltzmann equation, Hwang et al. (1996) proposed an adjustable slip model based on a modified high-order slip-flow velocity distribution. The slip model has three adjustable coefficients which are correlated to the Boltzman model. Li (2002, 2003) developed a complete database of Poiseuille flow rates and Couette flow rates by solving the linearized Boltzmann equation. Peng et al. (2004) investigated the unidirectional flow of rarefied gas between two parallel plates and proposed a nanoscale effect function that describes the influence of space restriction on gas lubrication between the slider and the disk. Using a linearized flow rate model (LFR), Shi and Yang (2010) derived a simplified Reynolds equation for ultra-thin gas film lubrication in HDDs.

In the following two sections, the authors will derive a simplified model of the Reynolds equation. Then the new model will be used to perform error analysis and numerical simulation to validate its accuracy and efficiency. In the second section, based on a Poiseuille flow rate database introduced in the FK model (Fukui and Kaneko 1990), a simplified precise second order (PSO) model is proposed and used to simulate ultra-thin gas film lubrication at the head/disk interface in HDDs. In the third section, the PSO model is evaluated using the finite volume method and the resultant numerical solutions are compared with other models, including the FK model.

$$
\begin{cases}
Q_p = D/6 + 1.0162 + 1.0653/D - 2.1354/D^2 & (5 \le D) \\
Q_p = 0.13852D + 1.25087 + 0.15653/D - 0.00969/D^2 & (0.15 \le D \le 5) \\
Q_p = -2.22919D + 2.10673 + 0.01653/D - 0.0000694/D^2 & (0.01 \le D \le 0.15)
\end{cases}
\tag{4}
$$

Then, the flow factor (Q) can be obtained by using Eqs. 3, 4, and the second equation of Eq. 1:

$$Q = \frac{Q_p(D, \alpha)}{Q_{con}(D)} = K_1 + K_2(PH)^{-1} + K_3(PH)^{-2} - K_4(PH)^{-3} \tag{5}$$

The corresponding coefficients for various inverse Knudsen numbers are shown in Table 1.

Substituting Eq. 5 into the first equation of Eq. 1, one can obtain the following equation:

$$\frac{d}{dX}\left[(K_1PH^3 + K_2H^2 + K_3P^{-1}H - K_4P^{-2})\frac{dP}{dX} - \Lambda_xPH\right]$$
$$+ \frac{d}{dY}\left[(K_1PH^3 + K_2H^2 + K_3P^{-1}H - K_4P^{-2})\frac{dP}{dY} - \Lambda_yPH\right] = 0 \tag{6}$$

Equation (6) is a non-linear differential equation. It is difficult and time-consuming to solve this equation using numerical methods.

The Poiseuille flow rate coefficients can be calculated numerically for various inverse Knudsen numbers (D) and accommodation coefficients (α). In this paper we will only consider the case of $\alpha = 1$. This corresponds to a case where gas molecules diffusely reflect at all surfaces. A database of the flow rate coefficients corresponding to $\alpha = 1$ are shown in Table 2 (Fukui and Kaneko 1990).

In order to further simplify the FK model of the Reynolds equation, the Poiseuille flow rate database is divided into eight intervals. Within each interval ($[d_i, d_j]$) the following continuous function ($\bar{Q}_p$) is implemented:

$$\bar{Q}_p = a + bD + cD^{-1} \quad d_i \leq D \leq d_j \tag{7}$$

where a, b, and c are unknown coefficients. At each interval, the values of a, b, and c are calculated as shown in Table 3 using the least squares method. Equation 7 has the same mathematical form in the other models including the first-order, second-order, and 1.5-order model.

Figure 2 compares Poiseuille flow rates calculated using different models. The flow rate calculated from the Boltzmann equation is included for reference. When compared to the flow rate calculated from the Boltzmann equation over a regime where the inverse Knudsen number varies from $D = 0.01$ to $D = 100$, the first-order slip-flow approximation under-estimates the flow rate while the second-order and 1.5th-order slip-flow approximations overestimate the flow rate. Using the model presented in this paper, we find a good approximation that is close to the flow rate calculated from the Boltzmann equation.

The flow factor Q of the simplified model is as follows and can be obtained by using Eqs. 3, 7, and the second equation of Eq. 1:

$$Q = A_1 + A_2\frac{K_n}{PH} + A_3\left(\frac{K_n}{PH}\right)^2 \tag{8}$$

Table 1 FK model coefficients for various inverse Knudsen numbers in the FK model

D	K_1	K_2	K_3	K_4
$0.15 \leq D < 5$	0.83112	$7.50522/D_0$	$0.93918/D_0^2$	$0.05814/D_0^3$
$5 \leq D$	1	$6.0972/D_0$	$6.3918/D_0^2$	$12.8124/D_0^3$
$0.01 \leq D < 0.15$	-13.37514	$12.64038/D_0$	$0.09918/D_0^2$	$0.0004164/D_0$

Table 2 Poiseuille flow database for $\alpha = 1$

Inverse Knudsen no. D	Flow rate Q_p	Inverse Knudsen no. D	Flow rate Q_p	Inverse Knudsen no. D	Flow rate Q_p	Inverse Knudsen no. D	Flow rate Q_p
100.0	17.693	9.0	2.608	0.8	1.548	0.07	2.167
90.0	16.028	8.0	2.449	0.7	1.559	0.06	2.228
80.0	14.363	7.0	2.292	0.6	1.576	0.05	2.302
70.0	12.698	6.0	2.134	0.5	1.602	0.04	2.397
60.0	11.033	5.0	1.991	0.4	1.641	0.035	1.454
50.0	9.370	4.0	1.846	0.35	1.668	0.03	2.522
40.0	7.708	3.5	1.777	0.3	1.703	0.025	2.604
35.0	6.878	3.0	1.711	0.25	1.748	0.02	2.707
30.0	6.049	2.5	1.649	0.2	1.808	0.015	2.846
25.0	5.222	2.0	1.595	0.15	1.895	0.01	3.060
20.0	4.398	1.5	1.554	0.1	2.033		
15.0	3.578	1.0	1.539	0.09	2.071		
10.0	2.768	0.9	1.542	0.08	2.115		

Table 3 PSO model coefficients for various inverse Knudsen numbers

D	A	B	C
$0.01 \leq D < 0.035$	2.6455	−9.7488	0.0051
$0.035 \leq D < 0.09$	2.1850	−2.8937	0.0130
$0.09 \leq D < 0.35$	1.7273	−0.4636	0.0350
$0.35 \leq D < 0.9$	1.4061	0.0428	0.0868
$0.9 \leq D < 3.5$	1.2745	0.1343	0.1295
$3.5 \leq D < 9.0$	1.0764	0.1647	0.4391
$9.0 \leq D < 35.0$	1.0421	0.1662	0.6347
$35.0 \leq D$	1.0202	0.1667	0.8848
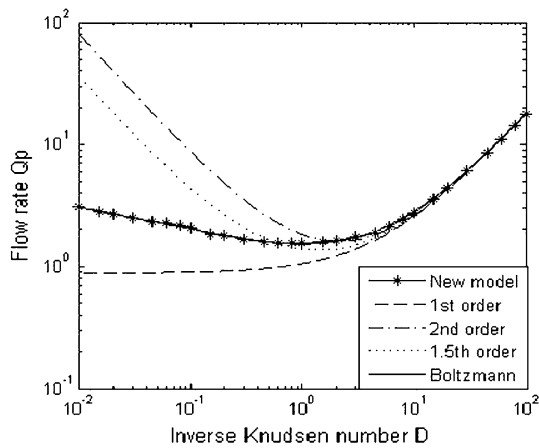
Fig. 2 Flow rate Q_p as function of inverse Knudsen number

Table 4 Coefficients used in Eqs. 8 and 9 for various inverse Knudsen numbers

D	A_1	A_2	A_3
$0.01 \leq D < 0.035$	−58.4929	17.9108	0.0390
$0.035 \leq D < 0.09$	−17.3621	14.7931	0.0993
$0.09 \leq D < 0.35$	−2.7816	11.6943	0.2674
$0.35 \leq D < 0.9$	0.2568	9.5197	0.6631
$0.9 \leq D < 3.5$	0.8059	8.6287	0.9893
$3.5 \leq D < 9.0$	0.9881	7.2875	3.3545
$9.0 \leq D < 35.0$	0.9972	7.0553	4.8488
$35.0 \leq D$	0.9999	6.9070	6.7594

where A_1, A_2 and A_3 are coefficients based on a, b and c in Eq. 7. K_n is the Knudsen number. The values of A_1, A_2, and A_3 are shown in Table 4.

Substituting Eq. 8 into Eq. 1, one obtains:

$$\frac{d}{dX}\left(\left(A_1 PH^3 + A_2 K_n H^2 + A_3 K_n^2 P^{-1} H\right)\frac{dP}{dX} - \Lambda_x PH\right) + \frac{d}{dY}\left(\left(A_1 PH^3 + A_2 K_n H^2 + A_3 K_n^2 P^{-1} H\right)\frac{dP}{dY} - \Lambda_y PH\right) = 0 \tag{9}$$
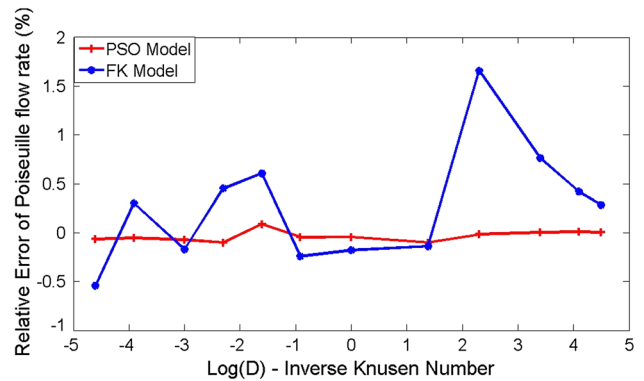
Fig. 3 Relative error of Poiseuille flow rate versus inverse Knudsen number for the PSO and FK model

This simplified model is called the "precise second order model", or PSO model. It is easy to see that the mathematical formulation of the PSO model is simpler than that of the FK model.

3 Error analysis and numerical examples

3.1 Error analysis

In order to compare the accuracy of the PSO model with the FK model, the relative errors of the two models are compared. The relative error E is defined as:

$$E_i = (X_i - Y)/Y \times 100\ \%\ (i = 1, 2) \tag{10}$$

where X_1 is the Poiseuille flow rate calculated using the FK model and X_2 is the flow rate calculated using the PSO model. Y is the corresponding flow rate from the database.

Figure 3 shows the relative errors of the Poiseuille flow rate for the two models versus the inverse Knudsen number. From Fig. 3, we observe that the relative error of the PSO model is less than that of the FK model and is very small across the whole domain. This indicates that the accuracy of the PSO model is better than that of the FK model.

3.2 Numerical examples

The two models, the PSO and FK models, were solved using the finite volume method in order to further compare their accuracy and computational efficiency.

Figure 4 shows pressure distributions for an infinitely long air bearing slider calculated using the PSO and FK models. For the calculation in Fig. 4, a film-thickness ratio $H_1 = h_2/h_1 = 2$, a Knudsen number $K_n = 1.25$, and bearing numbers of $\Lambda_x = 61.6$ and $\Lambda_x = 123.2$ were used. It is easy to see that the pressure distributions of the two models are in very good agreement with each other. The maximum

relative errors of the PSO and FK models are 0.0486 and 0.0492 %, respectively.

The pressure distribution of a tri-pad slider is shown in Fig. 5. Figure 6 shows the relative errors of the pressure profiles calculated using the PSO and FK models for the tri-pad slider. The flying attitude parameters of the tri-pad slider are listed in Table 5. The parameters α and β represent the pitch and roll angles, respectively, of the slider about the pivot point where the suspension is attached. δ denotes the skew angle at the radial position and is considered to be fixed.

Figure 6 shows that the relative errors of the pressure profiles calculated using the two models are very small for most of the air bearing surface. For the two models, the maximum relative error of the tri-pad slider is less than 3 %.

The computation times of the PSO and FK model for the tri-pad slider are listed in Table 6 for comparison. We can see that the computation time for the PSO model is a little
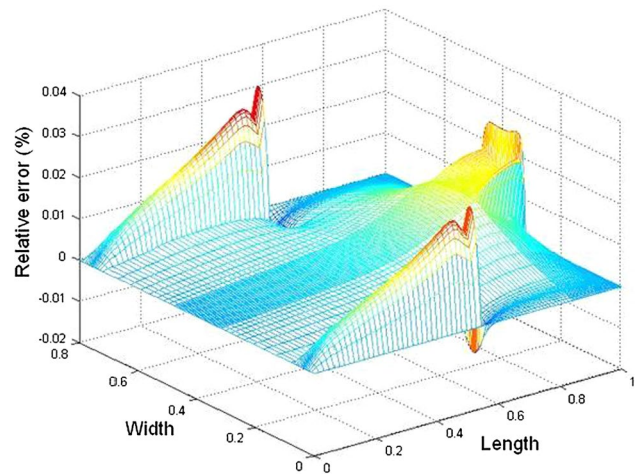

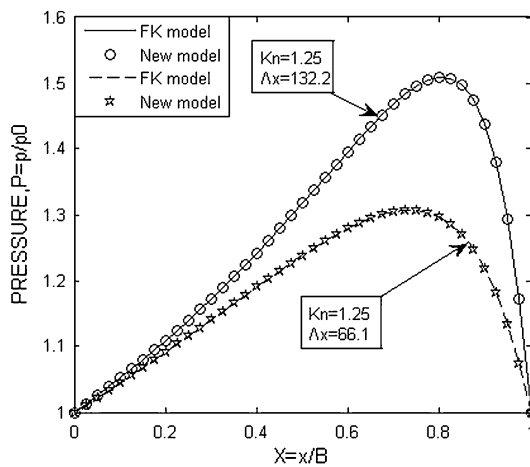**Fig. 6** Relative error of pressure for the PSO and FK model for typical tri-pad slider

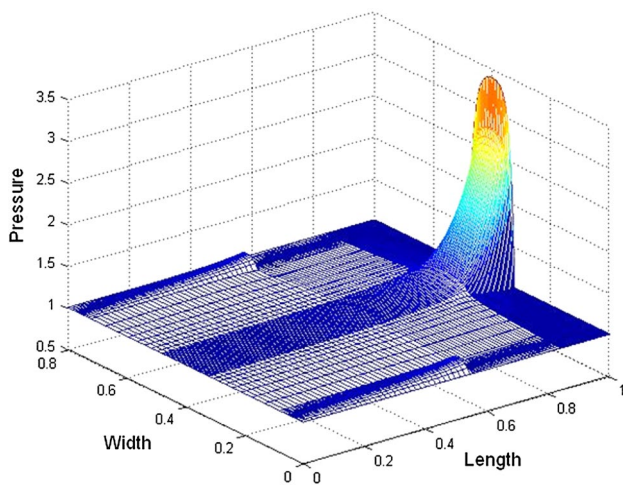**Fig. 4** Comparison of pressure distribution for an infinitely long air bearing slider for the PSO and FK model

Fig. 5 Non-dimensional pressure profile for typical tri-pad slider

Table 5 Flying attitude parameters of tri-pad slider

Minimum fling height (h_1)	40×10^{-9} m
Pitch angle (α)	300×10^{-6} rad
Roll angle (β)	0 rad
Skew angle (δ)	0 rad
Radial position	18×10^{-3} m
Rotate speed of the disk, RPM	7200

Table 6 Comparison of computation time for tri-pad slider using PSO and FK model

Slider type	Model type	Computation time (s)
Tri-pad slider	FK model	2194.241
	PSO model	2078.893

less than that of the FK model. In other words, the PSO model is slightly more computational efficient than the FK model.

4 Summary and conclusions

Starting from a Poiseuille flow rate database, we have proposed a simplified precise second order (PSO) model to simulate ultra-thin gas film lubrication at the head/disk interface in hard disk drives (HDDs). The PSO model is solved using the finite volume method. The numerical results are compared with other models, including the first-order model, the second-order model, and the widely used FK model. Numerical results show that the PSO model not

only has a simple mathematical formulation, but also possesses good accuracy and is computationally efficient.

References

Burgdorfer A (1959) The influence of the molecular mean free path on the performance of hydrodynamic gas lubricated bearings. ASME J Basic Eng 81:94–100

Fukui S, Kaneko R (1988) Analysis of ultra-thin gas film lubrication based on linearized Boltzmann equation: first report-derivation of a generalized lubrication equation including thermal creep flow. ASME J Tribol 110:253–262

Fukui S, Kaneko R (1990) A database for interpolation of Poiseuille flow rates for high Knudsen number lubrication problems. ASME J Tribol 112:78–83

Gans RF (1985) Lubrication theory at arbitrary Knudsen number. ASME J Tribol 107:431–433

Hsia YT, Domoto GA (1983) An experimental investigation of molecular rarefaction effects in gas lubricated bearings at ultra-low clearances. ASME J Tribol 105:120–130

Hwang CC, Fung RF, Yang RF, Weng CI, Li WL (1996) A new modified Reynolds equation for ultrathin film gas lubrication. IEEE Trans Magn 32(2):344–347

Juang JY, Bogy DB, Bhatia CS (2006) Alternate air bearing slider designs for areal density of 1 Tbit/in2. IEEE Trans Magn 42(2):241–246

Li WL (2002) A database for Couette flow rate considering the effects of non-symmetric molecular interactions. ASME J Tribol 124:869–873

Li WL (2003) A database for interpolation of Poiseuille flow rate for arbitrary Knudsen number lubrication problems. J Chin Inst Eng 26:455–466

Liu B, Yu S, Zhang M, Gonzaga L, Li H, Liu J, Ma Y (2007) Air-bearing design towards highly stable head-disk interface at ultra-low flying height. IEEE Trans Magn 43(2):715–720

Liu N, Zheng J, Bogy DB (2011) Thermal flying-height control sliders in air-helium gas mixtures. IEEE Trans Magn 47:100–104

Mitsuya Y (1993) Modified Reynolds equation for ultra-thin film gas lubrication using 1.5-order slip-flow model and considering surface accommodation coefficient. ASME J Tribol 115:289–294

Peng Y, Lu X, Luo J (2004) Nanoscale effect on ultrathin gas film lubrication in hard disk drive. ASME J Tribol 126:347–352

Salas PA, Talke FE (2013) Numerical simulation of thermal flying-height control sliders to dynamically minimize flying height variations. IEEE Trans Magn 49:1337–1342

Shi BJ, Yang TY (2010) Simplified model of Reynolds equation with linearized flow rate for ultra-thin gas film lubrication in hard disk drives. Microsyst Technol 16:1727–1734

Zheng H, Li H, Talke FE (2012) Numerical simulation of thermal flying height control sliders in heat-assisted magnetic recording. Microsyst Technol 18(9-10):1731–1739